



LJMU Research Online

Adekunle, YA, Samuel, BB, Oluyemi, WM, Adewumi, AT, Mosebi, S, Nahar, L, Fatokun, AA and Sarker, S

Oleanolic acid purified from the stem bark of *Olex subscorpioidea* Oliv. inhibits the function and catalysis of human 17 β -hydroxysteroid dehydrogenase 1

<http://researchonline.ljmu.ac.uk/id/eprint/23434/>

Article

Citation (please note it is advisable to refer to the publisher's version if you intend to cite from this work)

Adekunle, YA, Samuel, BB, Oluyemi, WM, Adewumi, AT, Mosebi, S, Nahar, L, Fatokun, AA and Sarker, S (2024) Oleanolic acid purified from the stem bark of *Olex subscorpioidea* Oliv. inhibits the function and catalysis of human 17 β -hydroxysteroid dehydrogenase 1. *Journal of Biomolecular Structure*

LJMU has developed **LJMU Research Online** for users to access the research output of the University more effectively. Copyright © and Moral Rights for the papers on this site are retained by the individual authors and/or other copyright owners. Users may download and/or print one copy of any article(s) in LJMU Research Online to facilitate their private study or for non-commercial research. You may not engage in further distribution of the material or use it for any profit-making activities or any commercial gain.

The version presented here may differ from the published version or from the version of the record. Please see the repository URL above for details on accessing the published version and note that access may require a subscription.

For more information please contact researchonline@ljmu.ac.uk

<http://researchonline.ljmu.ac.uk/>

ISSN: (Print) (Online) Journal homepage: www.tandfonline.com/journals/tbsd20

Oleanolic acid purified from the stem bark of *Olex subscorpioidea* Oliv. inhibits the function and catalysis of human 17 β -hydroxysteroid dehydrogenase 1

Yemi A. Adekunle, Babatunde B. Samuel, Wande M. Oluyemi, Adeniyi T. Adewumi, Salerwe Mosebi, Lutfun Nahar, Amos A. Fatokun & Satyajit D. Sarker

To cite this article: Yemi A. Adekunle, Babatunde B. Samuel, Wande M. Oluyemi, Adeniyi T. Adewumi, Salerwe Mosebi, Lutfun Nahar, Amos A. Fatokun & Satyajit D. Sarker (01 Nov 2024): Oleanolic acid purified from the stem bark of *Olex subscorpioidea* Oliv. inhibits the function and catalysis of human 17 β -hydroxysteroid dehydrogenase 1, Journal of Biomolecular Structure and Dynamics, DOI: [10.1080/07391102.2024.2423173](https://doi.org/10.1080/07391102.2024.2423173)

To link to this article: <https://doi.org/10.1080/07391102.2024.2423173>



© 2024 The Author(s). Published by Informa UK Limited, trading as Taylor & Francis Group



[View supplementary material](#)



Published online: 01 Nov 2024.



[Submit your article to this journal](#)



Article views: 346



[View related articles](#)



[View Crossmark data](#)

Oleanolic acid purified from the stem bark of *Olax subscorpioidea* Oliv. inhibits the function and catalysis of human 17 β -hydroxysteroid dehydrogenase 1

Yemi A. Adekunle^{a,b,c} , Babatunde B. Samuel^a , Wande M. Oluyemi^c , Adeniyi T. Adewumi^d , Salerwe Mosebi^d , Lutfun Nahar^e , Amos A. Fatokun^b  and Satyajit D. Sarker^b 

^aDepartment of Pharmaceutical Chemistry, Faculty of Pharmacy, University of Ibadan, Ibadan, Oyo State, Nigeria; ^bCentre for Natural Products Discovery, School of Pharmacy and Biomolecular Sciences, Liverpool John Moores University, Liverpool, UK; ^cDepartment of Pharmaceutical and Medicinal Chemistry, College of Pharmacy, Afe Babalola University, Ado-Ekiti, Ekiti State, Nigeria; ^dDepartment of Life and Consumer Sciences, University of South Africa, Florida, South Africa; ^eLaboratory of Growth Regulators, Palacký University and Institute of Experimental Botany, The Czech Academy of Sciences, Olomouc, Czech Republic

ABSTRACT

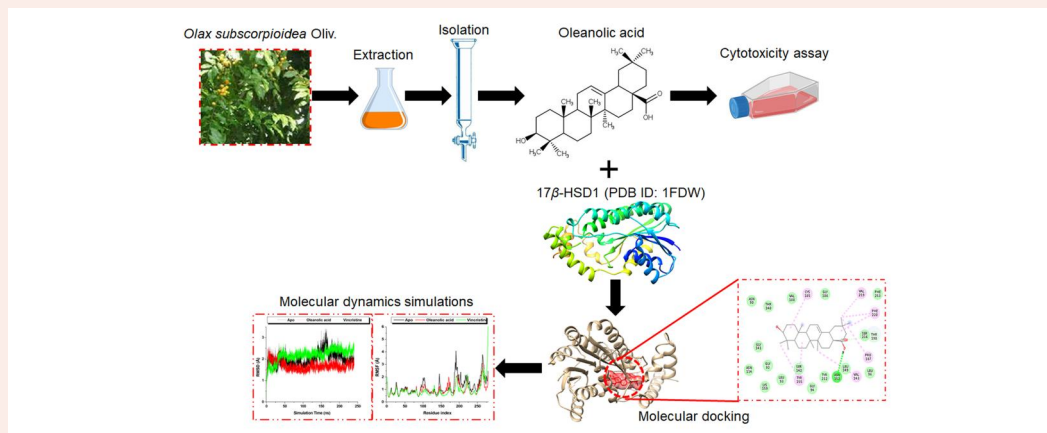
Cancer is a leading cause of global death. Medicinal plants have gained increasing attention in cancer drug discovery. In this study, the stem bark extract of *Olax subscorpioidea*, which is used in ethnomedicine to treat cancer, was subjected to phytochemical investigation leading to the isolation of oleanolic acid (OA). The structure was elucidated by 1-dimensional and 2-dimensional nuclear magnetic resonance spectroscopic (NMR) data, and by comparing its data with previously reported data. Molecular docking was used to investigate the interactions of OA with nine selected cancer-related protein targets. OA docked well with human 17 β -hydroxysteroid dehydrogenase type-1 (17 β HSD1), caspase-3, and epidermal growth factor receptor tyrosine kinase (binding affinities: -9.8 , -9.3 , and -9.1 kcal/mol, respectively). OA is a triterpenoid compound with structural similarity to steroids. This similarity with the substrates of 17 β HSD1 gives the inhibitor candidate an excellent opportunity to bind to 17 β HSD1. The structural and functional dynamics of OA-17 β HSD1 were investigated by molecular dynamics simulations at 240 ns. Molecular mechanics/Poisson-Boltzmann surface area (MMPBSA) studies showed that OA had a binding free energy that is comparable with that of vincristine (-52.76 , and -63.56 kcal/mol, respectively). The average C- α root mean square of deviation (RMSD) value of OA (1.69 Å) compared with the unbound protein (2.01 Å) indicated its high stability at the protein's active site. The binding energy and stability at the active site of 17 β HSD1 recorded in this study indicate that OA exhibited profound inhibitory potential. OA could be a good scaffold for developing new anti-breast cancer drugs.

ARTICLE HISTORY

Received 20 January 2024
Accepted 4 June 2024




KEYWORDS


Olax subscorpioidea; oleanolic acid; 17 β -hydroxysteroid dehydrogenase-1; breast cancer; nuclear magnetic resonance; molecular docking; molecular dynamics simulations



HIGHLIGHTS

- Oleanolic acid has been isolated from the cytotoxic fraction of *Olax subscorpioidea* stem bark extract. Its structure was deduced by 1D- and 2D-NMR analyses.
- The compound has strong interaction with human 17 β -hydroxysteroid dehydrogenase-1 (PDB: 1FDW), caspase-3 (PDB: 1GFV), epidermal growth factor receptor tyrosine kinase (PDB: 5JEB), and poly(ADP-ribose) polymerase-1 (PDB: 5DS3), with binding affinities of -9.8 , -9.3 , -9.1 , and -8.9 kcal/mol, respectively.

CONTACT Yemi A. Adekunle  y.a.adekunle@2022.ljmu.ac.uk; Babatunde B. Samuel  bb.samuel@mail.ui.edu.ng; Lutfun Nahar  nahar@ueb.cas.cz

 Supplemental data for this article can be accessed online at <https://doi.org/10.1080/07391102.2024.2423173>.

© 2024 The Author(s). Published by Informa UK Limited, trading as Taylor & Francis Group

This is an Open Access article distributed under the terms of the Creative Commons Attribution-NonCommercial-NoDerivatives License (<http://creativecommons.org/licenses/by-nc-nd/4.0/>), which permits non-commercial re-use, distribution, and reproduction in any medium, provided the original work is properly cited, and is not altered, transformed, or built upon in any way. The terms on which this article has been published allow the posting of the Accepted Manuscript in a repository by the author(s) or with their consent.

- MMPBSA studies, C- α RMSD and other MD parameters supported the inhibitory potential of oleanolic acid against critical residues involved in the catalysis of 17 β -hydroxysteroid dehydrogenase-1.

Abbreviations: AMBER: *Assisted Model Building with Energy Refinement* ; Apo: Ligand free; ATCC: American Type Culture Collection; BFE: Binding free energy; Caco-2: Human colorectal cancer cell line; COSY: Homonuclear correlation spectroscopy; DEPTQ: Distorsionless enhancement by polarisation transfer including quaternary nuclei; DMEM: Dulbecco's Modified Eagle Medium; FBS: Foetal bovine serum; FRIN: Forestry Research Institute of Nigeria; FTIR: Fourier transform infrared spectroscopy; ΔG : Gibb's free energy; GPU: Graphics processor unit; HeLa: Human cervical cancer cell line; 17 β HSD1: Human 17 β -hydroxysteroid dehydrogenase type 1; HSQC: Heteronuclear single quantum coherence; HMBC: Heteronuclear multiple bond correlation; μ M: Micromolar; MMPBSA: Mechanics/Poisson-Boltzmann surface area; MCF-7: Human breast adenocarcinoma cell line; MD: Molecular dynamics; MTT: 3-[4,5-dimethylthiazole-2-yl] 3,5-diphenyltetrazolium bromide; NMR: Nuclear magnetic resonance; NOESY: Nuclear overhauser effect spectroscopy; OA: Oleanolic acid; PCA: Principal component analysis; PDB: Protein data bank; PMEMD: Particle mesh Ewald molecular dynamics; PRED: Per-residues energy decomposition; 1 H NMR: Proton nuclear magnetic resonance; RD: Rhabdomyosarcoma; RoG: Radius of gyration; RMSD: Root mean square of deviation; RMSF: Root mean square of fluctuation; SASA: Solvent accessible surface area

1. Introduction

Cancer is a noncommunicable disease that causes more deaths globally than human immunodeficiency virus/acquired immunodeficiency syndrome (HIV/AIDs) (Sung et al., 2021). It is a leading cause of mortality in almost every World Health Organisation region of the world (Wild et al., 2020). Current chemotherapeutic agents have significantly helped in the management of different types of cancer. However, they are often plagued with several limitations such as adverse effects and resistance (Gyanani et al., 2021). Natural products and their derivatives have contributed significantly to the development of cancer drugs (Newman & Cragg, 2020; Sarker et al., 2020) and they continue to receive increasing attention for anticancer drug discovery (Abdelrheem et al., 2021).

Olex subscorpioidea Oliv. (Olacaceae) is an ethnomedicinally important plant used to treat various diseases (Adekunle, Samuel, Akinleye, et al., 2022; Agbabiaka & Adebayo, 2021; Tsakem et al., 2022). Its indications among local users include its use in the treatment of cancer (Soladoye et al., 2010), convulsion (Nazifi et al., 2015), diabetes mellitus (Olabanji et al., 2014), malaria (Kipre et al., 2015), worm infections and venereal diseases (Olowokudejo et al., 2008). Ethnobotanical studies have shown that *O. subscorpioidea* is used to treat cancer in Nigeria (Gbadamosi & Erinoso, 2016). The aim of this study therefore is to isolate the anticancer principle(s) from the stem bark extract of *O. subscorpioidea*. Adekunle, Samuel, Fatokun, et al. (2022) investigated the anticancer effects of the root and stem bark extracts of *O. subscorpioidea* against human breast cancer (MCF-7) and rhabdomyosarcoma (RD) cell lines. Triterpenes and their glycosides (Adekunle et al., 2023; Forgacs & Provost, 1981; Pertuit et al., 2018; Sule et al., 2011; Vo et al., 2019), sesquiterpenes (Nguyen et al., 2019), and flavonoids and their glycosides (Okoye et al., 2015, 2016) have been isolated from the plants of the genus *Olex* plants.

Recently, α -amyirin, β -sitosterol, and stigmasterol were isolated from the stem bark of this plant. In addition, more than twenty other compounds were identified by tandem mass spectrometric (MS/MS) analysis of the plant extract using the Global

Natural Products Social Molecular Networking (GNPS) (Oladipupo et al., 2023). Chemical investigation of the ethanol extract of *O. subscorpioidea* stem bark afforded five compounds, including three previously undescribed flavonoid glycosides (Tsakem, Tchuenguem, et al., 2023). A rotameric biflavonoid glycoside, together with known 4'-O- methylgallo catechin was isolated from the stem bark (Tsakem, Toussie, et al., 2023).

Human 17 β -hydroxysteroid dehydrogenase type 1 (17 β HSD1) catalyses the last step in the conversion of estrone (less active oestrogen) to 17 β -oestradiol (more active oestrogen) (Ghosh et al., 1995). Oestradiol is a biologically active oestrogen implicated in human breast cancer cell proliferation (Mazza et al., 1998). Blocking the synthesis of 17 β -oestradiol could arrest the proliferation of breast cancer cells (Aka et al., 2010; Frotscher et al., 2008; Ghosh et al., 1995). Important tyrosine¹⁵⁵ (TYR155), serine¹⁴² (SER142) and lysine¹⁵⁹ (LYS159) residues in the hydrophobic substrate-binding site have been identified to play critical roles in the catalytic functions of the enzyme (Mazza et al., 1998). As reported by Puranen et al. (1994), mutation of TYR155 to an alanine residue led to almost total loss of catalysis by 17 β HSD1. TYR155-mutated 17 β HSD1 also preferentially catalysed oxidation reaction *in vitro* more than reductive reaction (Puranen et al., 1994). This attests to the significance of TYR155 as a critical residue in the catalytic function of the enzyme.

An analysis of 17 β HSD1's crystal structure with oestradiol provided insights into the mechanism by which it recognizes oestrogen. Oestradiol and the active site have a high complementarity (Azzi et al., 1996). Histidine221/Glutamic acid282 forms one end of the hydrophobic tunnel substrate-binding site, while Serine142/Tyrosine155 (along with Asparagine114 and Lysine159) forms the other end (Frotscher et al., 2008). A hydrogen bond is formed between these amino acids and the hydroxyl groups of oestradiol at C-3 and C-17, respectively (Ayan et al., 2012; Frotscher et al., 2008; He et al., 2016). Researchers have developed several compounds that inhibit the 17 β HSD1 enzyme, and one steroidal compound (OG-6219) has recently entered the clinical phase for endometriosis and breast cancer (Poirier et al., 2022; Rizner & Romano, 2023; Xanthoulea

et al., 2021). By understanding the structure of the substrate-binding site, it is possible to design more specific inhibitors of this estrogenic enzyme for breast cancer treatment (Ghosh et al., 1995). Human 17β HSD1 is a promising target for developing hormone-dependent diseases, including breast cancer (Lilienkampf et al., 2009). Steroidal compounds STX1040 (Day et al., 2008) and PBRM (Ayan et al., 2012) and non-steroidal compounds (Starčević et al., 2011) have been developed as inhibitors of 17β HSD1 enzyme. Flavonoids and cinnamic acid derivatives (Brožič et al., 2009) have shown inhibitory potential against 17β HSD1. In addition, 3-phenylcoumarin analogues (Niinivehmas et al., 2018) and (hydroxyphenyl)naphthalene and quinoline derivatives (Frotscher et al., 2008) have been synthesised to block the biosynthesis of oestradiol via 17β HSD1 inhibition. Although some inhibitors of 17β HSD1 are now being used in preclinical and clinical phases, no inhibitors of the enzyme have been approved for cancer treatment.

Molecular docking is a computational technique that predicts the binding of drug-like small molecules to protein receptors (Ainsley et al., 2018), while molecular dynamics simulations offer uniqueness in capturing the interactions and behaviours of proteins and other biomolecules in full atomic detail (Hollingsworth & Dror, 2018). These techniques have been extensively used in studying the molecular mechanisms of actions of compounds isolated from medicinal plants against relevant protein targets (Moumbock et al., 2019; Oluyemi et al., 2022; Rathod et al., 2023). The aim of this study was to isolate bioactive compound(s) from the cytotoxic fraction of *O. subscorpioidea* stem bark, and to study the interactions of the isolated compound(s) against selected cancer-related protein targets via molecular docking and molecular dynamics simulations studies.

2. Materials and methods

2.1. Materials

Methanol and water (Fisher Chemical, Loughborough, United Kingdom), ethyl acetate (Thermo Scientific, Germany), Dulbecco's Modified Eagle Medium (UK), fetal bovine serum (Sigma-Aldrich, U.S.A), Gibco's trypLE Express (1X) (UK), Dulbecco's phosphate buffered-saline, MTT (3-(4,5-dimethylthiazol-2-yl)-2,5-diphenyl-2H-tetrazolium bromide) (Sigma-Aldrich, U.S.A), Tocris' vinblastine (Abingdon, UK), antibiotic-antimycotic (100X) (Gibco, U.S.A), L-glutamine 200 mM (100X) (Gibco, UK), Strata C-18 cartridge (35 μ m; 70 \AA ; 20 g, Phenomenex), open glass chromatography (35 cm \times 3 cm), rotary evaporator R-100 rotavapor (BUCHI, Switzerland), Cary 630 FTIR spectrophotometer (Agilent Technologies, USA), Bruker Avance III NMR spectrometer at 600 MHz (Massachusetts, U.S.A), Tecan Spark 10 M multimode microplate reader (Switzerland).

2.2. Plant collection

The stem bark of *O. subscorpioidea* was collected by a taxonomist at the Forestry Research Institute of Nigeria (FRIN),

Ibadan in November 2021. The herbarium sample was deposited at Forest Herbarium Ibadan (FHI) with a voucher number FHI113182. The plant sample was washed, peeled, and air-dried for about 10 days before being pulverised.

2.3. Extraction and isolation

About 310 g of the plant powder was subjected to Soxhlet extraction using 1.5 L of methanol. The fraction was then concentrated with a rotary evaporator RE52-1 (Searchtech Instruments, England). About 62.5 g of crude extract was obtained. A portion (4 g) of the extract was subjected to solvent partitioning into methanol and *n*-hexane (250 mL each) inside a separating funnel. Each layer was carefully collected and concentrated with a rotary evaporator R-100 rotavapor (BUCHI, Switzerland). Approximately 2 g of the methanol fraction was further treated with solid-phase extraction to obtain four sub-fractions (Cartridge, Strata C-18; 35 μ m; 70 \AA ; 20 g, Phenomenex). The cartridge was eluted with 20%, 50%, 80%, and 100% methanol in water to obtain sub-fractions OSS1, OSS2, OSS3, and OSS4, respectively. OSS4 showed the highest activity when tested against the human cervical cell line (HeLa). OSS4 (45 mg) was subjected to column chromatography using silica gel 60-200 mesh packed with *n*-hexane. Gradient mobile phase was used: 90/10%, 80/20%, 70/30%, 50/50%, 40/60%, 30/70%, 20/80%, 10/90%, 0/100% *n*-hexane/ethyl acetate. About 30 fractions of approximately 3 mL each were obtained. Fractions 1 to 6 were pooled together, containing a single compound (called OSS4a in this study), a white amorphous sample (2.3 mg).

2.4. In vitro MTT assay

2.4.1. Cell line and cell culture

The cell line used for this study (human cervical cell line, HeLa) was originally obtained from the American Type Culture Collection (ATCC). The cells were grown in Dulbecco's Modified Eagle Medium (DMEM) supplemented with 10% foetal bovine serum (FBS), 1% 2 mM L-glutamine, and 1% penicillin-streptomycin solution, and kept in an incubator at 37 °C in a humidified atmosphere of 5% CO₂. Passaging was done bi-weekly. A cell density of 7.5×10^3 cells/well was used. Ninety-six-well microplates seeded with cells were incubated for 24 h before experiments. Cells were visualised with an inverted microscope (Olympus CKX41, UK).

2.4.2. MTT cytotoxicity assay

The cytotoxic effects of fractions OSS1, OSS2, OSS3, and OSS4 against the HeLa cell line were assessed by 3-[4,5-dimethylthiazole-2-yl] 3,5-diphenyltetrazolium bromide (MTT) *in vitro* assay as previously reported (Mosmann, 1983). After 24 h of incubation, cells were treated with 1, 10, 50, 100, 200 and 500 μ g/mL concentrations of the fractions. Stock solutions were made in DMSO and all dilutions were made in full growth medium (containing not more than 0.1% DMSO)

(Adekunle et al., 2023). The experiment was performed in triplicate and percentage cell viability was determined.

2.5. Spectral analysis

The following experiments were carried out on a 600 MHz Avance III NMR spectrometer (Bruker, Massachusetts, USA): ^1H , ^{13}C -DEPT-Q, COSY, HSQC, HMBC, and NOESY. Fourier transform infrared spectroscopy (FTIR) was carried out on Cary 630 FTIR spectrophotometer (Agilent Technologies, USA).

2.6. Statistical analysis

The results were represented as mean of $\text{IC}_{50} \pm \text{SEM}$. GraphPad Prism version 9.4.0 was used to determine the IC_{50} values. One-way ANOVA followed with Dunnett's post hoc established the level of statistical significance ($p < 0.05$).

2.7. Molecular docking

2.7.1. Proteins retrieval and preparation

Nine cancer-related proteins were retrieved from the protein data bank (PDB) (Berman et al., 2000) (<http://rcsb.org/>). The proteins are 17β -hydroxysteroid dehydrogenase type 1 (PDB ID: 1FDW) (Mazza et al., 1998), caspase-3 (PDB ID: 1GFW) (Lee et al., 2000), epidermal growth factor receptor tyrosine kinase (PDB ID: 5JEB) (Novotny et al., 2016), poly(ADP-ribose) polymerase-1 (PDB ID: 5DS3) (Dawicki-McKenna et al., 2015), $\alpha\beta$ -tubulin (PDB ID: 1JFF) (Löwe et al., 2001), phosphoinositide 3-kinase (PDB ID: 1E8Z) (Walker et al., 2000), bromodomain-containing protein 4 (PDB ID: 7JKW) (Li et al., 2020), human oestrogen receptor alpha (PDB ID: 3ERT) (Shiau et al., 1998), and polo-like kinase 1 (PDB ID: 3FC2) (Rudolph et al., 2009). Co-crystallised ligands, water and ion molecules, and other molecules were removed (Thomsen & Christensen, 2006) from the proteins' structures using UCSF Chimera tool (1.16) (Pettersen et al., 2004). Hydrogen was added to help in finding hydrogen bond interaction between protein and ligand. Partial atomic charges were added to the ligands by Gasteiger forcefield because the PDB structure lacks it (Mucs & Bryce, 2013). Energy minimisation was carried out on all proteins and OA (Oluyemi et al., 2022). The 3D structure of oleanolic acid (OA) was retrieved from PubChem (<https://pubchem.ncbi.nlm.nih.gov/>) (ID: 10494).

2.7.2. Docking analysis

Site-directed docking of OA on the active sites of the proteins was carried out using AutoDock Vina in the Python Prescription Virtual Screening Tool (PyRx) (Trott & Olson, 2010). On the graphics processing unit (GPU) of PyRx, OA was minimised and then converted to AutoDock ligand while the proteins were made macromolecules. The proteins' active sites were defined as their zones within 5 Å of the co-crystallised ligands. The key residues identified in the active site of 17β HSD1 include SER142, VAL143, GLY144, MET147, LEU149, TYR155, GLY186, PRO187, TYR218, GLN221, SER222, VAL225,

PHE226, PHE259, LEU262, MET279, GLU282, and VAL283. Grid boxes were set to fit the proteins' active sites. Docking scores (highest negative energy in kcal/mol) were determined, and docked poses were visualised using BIOVIA Discovery Studio Visualizer 2021 client (Adewumi et al., 2023).

2.8. Molecular dynamics simulations

Molecular dynamics (MD) simulation was performed using the GPU version of the PMEMD.CUDA engine (Lee et al., 2017) provided with the AMBER package, FF18SB variant of the AMBER forcefield used to describe the protein (Case et al., 2018). ANTECHAMBER was used to add partial charges to the ligand and AMBER18's LEAP module was run to add H^+ , Na^+ and Cl^- counter ions to neutralize and solvate Apo and bound systems (Olanlokun et al., 2019). All systems (Apo, Apo-OA, and Apo-vincristine) were solvated in an orthorhombic TIP3P water box of a size of 10 Å (Harrach & Drossel, 2014). Minimization steps were carried out on all systems: First 2500 steps preliminary minimization using a weak restraint potential of 10 kcal/mol. Then a 2500 full minimization (conjugate energy not restrained) (Oladipo et al., 2024). The systems were gradually heated from 0 to 300 K for 5 ps in a canonical ensemble (NVT), using harmonic restraint of 10 kcal/mol and a Langevin thermostat with a 1 ps random collision frequency. The systems were also equilibrated at 300 K, in an isothermal-isobaric (NPT) ensemble for 1 ns of a time step of 2 fs without any restraint using the Berendsen-Barostat to maintain the systems' pressure at 1 bar (Berendsen et al., 1984). The systems were set up for molecular dynamics simulations. Production MD was run for all systems for 240 ns. Simulation trajectories such as C- α root mean square of deviation (RMSD) (Lee et al., 2017), root mean square of fluctuation (RMSF) (Dong et al., 2018), radius of gyration (RoG) (Lobanov et al., 2008), principal component analysis (PCA) (Post et al., 2019), trajectory snapshots (Oluyemi et al., 2022), and solvent-accessible surface area (SASA) (Roe & Cheatham, 2013) were obtained. These MD parameters will help in capturing the detailed atomic interactions between the protein and the ligand (Adewumi et al., 2023; Hollingsworth & Dror, 2018; Oluyemi et al., 2022). Post-MD data analysis was done on Microcal Origin (6.0) graphic and data analysing tool (Oluyemi et al., 2022). Thermodynamic binding free energy (BFE) and per-residues energy decomposition (PRED) were determined by the molecular mechanics/Poisson-Boltzmann surface area (MMPBSA) method (Wang et al., 2019). Thermodynamics calculations were done as follows:

$$\begin{aligned}\Delta G_{\text{bind}} &= \Delta G_{\text{complex}} - \Delta G_{\text{receptor}} - \Delta G_{\text{ligand}} \\ \Delta G_{\text{bind}} &= E_{\text{gas}} + G_{\text{sol}} - T\Delta S \\ E_{\text{gas}} &= E_{\text{int}} + E_{\text{vdw}} + E_{\text{ele}} \\ G_{\text{sol}} &= G_{\text{GB}} + G_{\text{SA}} \\ G_{\text{SA}} &= \text{SASA}\end{aligned}$$

ΔG_{bind} is the gas-phase summation. G_{sol} is solvation free energy. $-T\Delta S$ is conformational entropy upon ligand binding. E_{gas} is the gas-phase energy. ΔE_{int} is internal energy. ΔE_{ele} is electrostatic energies. ΔE_{vdw} is van der Waals energies. SA is

non-polar solvation energy. SASA is solvent-accessible surface area (Wang et al., 2019).

3. Results and discussion

3.1. Structure elucidation

OSS4a was isolated as a white amorphous powder. The FTIR spectrum showed peaks at 3300 cm^{-1} (OH stretching); 2970 and 2900 cm^{-1} (CH stretching); and 1680 cm^{-1} (C=O). Proton (^1H) NMR spectrum showed upfield signals for seven tertiary methyl groups: δ_{H} 0.97 (CH₃-23), 0.77 (CH₃-24), 0.94 (CH₃-25), 0.81 (CH₃-26), 1.16 (CH₃-27), 0.90 (CH₃-29), and 0.94 (CH₃-30). The positions of the methyl groups were determined by HSQC and HMBC experiments. An oxy-methine signal at δ_{H} 3.14 *dd* (3.1, 10.6 Hz, H-3) which had COSY correlation with a methylene at 1.60 *m* (H-2), and one olefinic proton signal at δ_{H} 5.24 *t* (H-12) were also observed. The olefinic proton had a COSY correlation with a methylene at 1.92 *m* (H-11). Seven corresponding tertiary methyl groups were observed in the ^{13}C -DEPT-Q NMR spectrum: δ_{C} 27.3 (C-23), 14.9 (C-24), 14.5 (C-25), 16.3 (C-26), 25.0 (C-27), 32.2 (C-29), and 22.6 (C-30). An oxy-methine carbon signal was observed at δ_{C} 78.3 (C-3). An olefinic carbon δ_{C} 122.2 and a trisubstituted carbon δ_{C} 143.8 were also observed. In the NOESY spectrum, correlations were observed between H-3 (3.14)/H-5 (0.75), and H-5/H-9 (1.60), indicating their α -axial configurations, hence the β -orientation of the hydroxyl unit at C-3 (Aouane et al., 2022). The 1D and 2D NMR data of OSS4a agreed with those we recently reported in the root extract of *O. subscorpioidea* for oleanolic acid (Adekunle et al., 2023) (Figure 1). The data also agreed with the literature values for oleanolic acid (Mahato & Kundu, 1994; Seebacher et al., 2003). To the best of our knowledge, this is the first report of the isolation and NMR analysis of OA from *O. subscorpioidea* stem bark.

3.2. In vitro cytotoxicity assay

The current study is a continuation of the previous studies conducted in our lab. We had reported that the stem bark

extract of *O. subscorpioidea* gave IC₅₀ values of $4.79 \pm 0.43\ \mu\text{g/mL}$ and $176.16 \pm 1.12\ \mu\text{g/mL}$ against rhabdomyosarcoma and MCF-7, respectively (Adekunle, Samuel, Fatokun, et al., 2022). In addition, we reported the isolation of OA from the root of *O. subscorpioidea* and its cytotoxic effects against human colorectal cancer cell line (Caco-2) (IC₅₀: $62.92 \pm 0.82\ \mu\text{M}$), human breast cancer cell line (MCF-7) (IC₅₀: $66.63 \pm 8.76\ \mu\text{M}$), and human cervical cancer cell line (HeLa) (IC₅₀: $110.21 \pm 15.64\ \mu\text{M}$). Vincristine was used as the positive control with the IC₅₀ values ranging from $0.54 \pm 0.06\ \mu\text{M}$ to $1.42 \pm 0.40\ \mu\text{M}$ against the three cancer cell lines (Adekunle et al., 2023). In the present study, bioactivity-guided isolation of a cytotoxic compound from the stem bark of *O. subscorpioidea* was conducted. The SPE fractions of the methanol crude extract were tested against HeLa cell line. The results showed that fraction 4 (OSS4) had the highest activity with an IC₅₀ value of $53.74667 \pm 4.97\ \mu\text{g/mL}$ (Table 1, Figure 2, and Supplementary material, Figure S8). All values were normalised to the full growth medium (negative control). Therefore, OSS4 was further subjected to chromatographic purification. This led to the isolation of its cytotoxic constituent which was characterised by 1D- and 2D-NMR analyses as oleanolic acid (OA). Our lab recently reported the cytotoxicity of OA against three cancer cell lines including HeLa (Adekunle et al., 2023). There are many other reports on the anticancer potential of OA (Feng et al., 2009; Parikh et al., 2014). OA isolated from *Glossogyne tenuifolia* (Labill.). Cass. Ex Less. has been reported to exhibit weak cytotoxic effects against breast cancer cell lines (MCF-7 and

Table 1. Cytotoxic effects of fractions OSS1 to OSS4 on HeLa cell line. Vincristine was used as a reference drug. The data are presented as mean \pm SEM (representative single run, in triplicate).

Fractions	IC ₅₀ \pm SEM ($\mu\text{g/mL}$ or μM for vincristine*)
OSS1	122.04 \pm 38.62
OSS2	106.18 \pm 37.04
OSS3	228.40 \pm 16.84
OSS4	53.74 \pm 4.97
Vincristine	1.42 \pm 0.40*

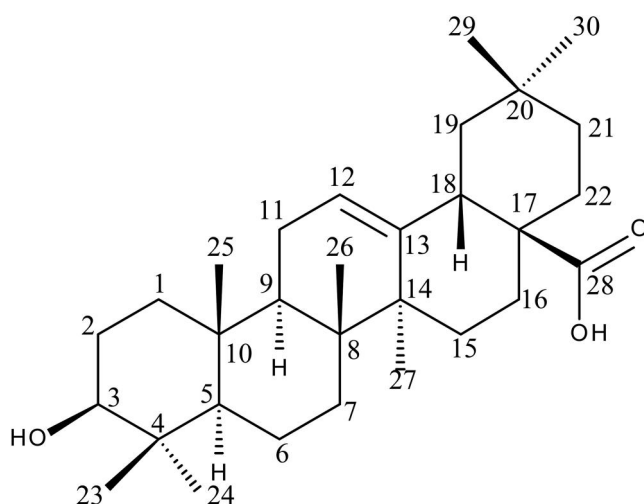


Figure 1. Structure of OSS4a isolated from the stem bark of *O. subscorpioidea*.

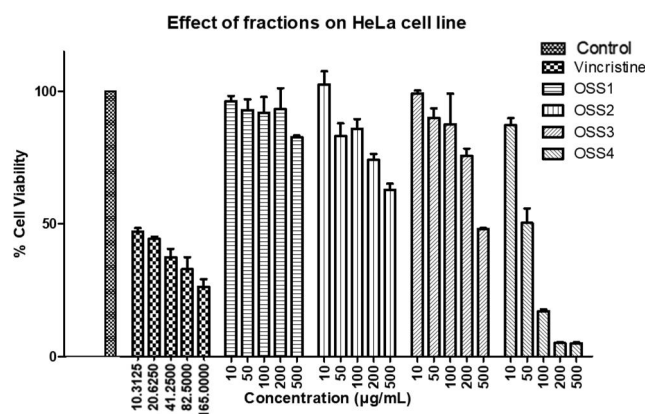


Figure 2. Effects of solvent fractions of *O. subscorpioidea* stem bark on HeLa cell line (representative single run in triplicate – error bars are for the triplicate readings). Vincristine was used as positive control. Full Growth Medium was used as negative control (DMEM containing 10% FBS, 1% 2 mM L-glutamine, and 1% penicillin-streptomycin solution).

MDA-MB-231) (Hsu et al., 2005). Yan et al. (2010) investigated the apoptotic induction effects of OA on four human cancer cell lines (HepG2, Hep3B, Huh7 and HA22T). At 2, 4, and 8 $\mu\text{mol/L}$, OA concentration-dependently lowered cell viability and enhanced DNA fragmentation in HepG2 and Hep3B cell lines. Reduction in cell viability and increase in DNA fragmentation was only observed at 4 and 8 $\mu\text{mol/L}$ in Huh7 cell. OA treatment also reduced mitochondrial membrane potential in HepG2, Hep3B and HA22T cell lines, reduced Na^+/K^+ -ATPase activity and vascular endothelial growth factor levels in all the cell lines, and elevated the activities of caspase-3 and caspase-8 in HepG2, Hep3B, and HA22T cell lines (Yan et al., 2010). Recently, Rasheed et al. (2023) isolated OA from *Lavandua stoechas* L. which showed cytotoxic effects against MCF-7 and MDA-MB-231. In addition, the study demonstrated increased caspase-9 and caspase-7 activities in OA-treated MCF-7 cells, as well as down-regulation of the B-cell lymphoma 2 (Bcl2) and platelet-derived growth factor (PDGF) genes.

3.3. Computational analyses

3.3.1. Molecular docking

Molecular docking predicts the most predominant and favourable binding modes of a ligand in the binding pocket of a protein (Tripathi & Bankaitis, 2017). In addition to the *in vitro* anticancer activity of OA from *O. subscorpioidea* root reported in a previous study (Adekunle et al., 2023), a multi-protein target screening approach was employed to investigate the anticancer potential of the inhibitor candidate from the stem bark *via* molecular docking. The proteins were selected based on good resolutions (1.5–2.5 Å) and species (human crystallised protein targets/protein targets of animals close to human physiology and anatomy). Other selection criteria include the method of crystallisation, R-value, and sequence identity and similarity. The docking scores of OA with nine cancer protein targets were recorded in Table 2. The proteins are largely expressed in breast cancer cells. 17 β HSD1 is overexpressed in breast cancer (Frotscher et al., 2008), EGFR tyrosine kinase is expressed in many cancers, including lung, brain, and breast cancers (Uribe et al., 2021; Weinberg et al., 2020), and caspase-3 is also expressed in many cancers, including gastric, breast, and colorectal cancers (Huang et al., 2018). The highest binding energy was observed in 17 β HSD1 with a binding affinity of -9.8 kcal/mol (Table 2). This is followed by caspase-3 (-9.3 kcal/mol) and epidermal growth factor receptor (EGFR) tyrosine kinase (-9.1 kcal/mol). By indication, the investigated compound bound most favourably with 17 β HSD1 in its binding site compared to other protein targets. Hence, 17 β HSD1, when compared to other screened protein targets, is considered the most suitable target to investigate the inhibitory potential of OA against the proliferation of human breast cancer

cells (Aka et al., 2010; Starčević et al., 2011). The amino acid residues that were involved in OA-17 β HSD1 binding essentially by hydrophobic interactions include GLY13, GLY15, ASN90, GLY92, THR140, SER142, LEU149, ASN152, TYR155, LYS159, GLY186, VAL188, THR190, VAL225. OA bound to caspase-3 *via* hydrophobic interaction, with the involvement of LEU168, SER205, ARG207, PHE250, SER251, PHE252, PHE256, and with TYR204 and TRP 206 *via* pi-sigma interaction. OA and EGFR tyrosine kinase interaction occurred *via* LYS695, ALA698, VAL702, ALA719, LYS721, LEU768, CYS773, LEU775, ASP776, LEU820, ARG817, and THR820. Due to the strong binding affinity of OA against 17 β HSD1, this enzyme was therefore further investigated by molecular dynamics simulations.

3.4. Molecular dynamics simulations

3.4.1. Binding free energy calculations, receptor-ligand interaction, and per-residue energy

The binding free energy and per-residue energy decomposition calculations were performed in the first 40 ns (0–40 ns) of the 240 ns simulation time (Oluyemi et al., 2022). Using MMPBSA method, the binding free energy of OA-17 β HSD1 was determined to be -52.76 ± 0.11 kcal/mol relative to that of vincristine-17 β HSD1 determined to be -63.56 ± 0.22 kcal/mol (Table 3). This indicates that the energy of binding of OA with the receptor is comparable with that of the reference anticancer drug. This explains the stability of OA on the binding pocket of 17 β HSD1. In addition, the binding free energy of oestradiol-17 β HSD1 (co-crystallised ligand) was computed to be -37.68 ± 0.22 kcal/mol (Table 3). This shows better conformational interactions of OA-17 β HSD1 system compared to the oestradiol-17 β HSD1 system. The current work was run for a 240 ns simulation time and eight key interacting residues with OA which contributed to the binding free energy (-52.76 ± 0.11 kcal/mol) were identified; they include VAL143, ASN152, TYR155, CYS185, PRO187, THR190, VAL219, and PHE220 (Figure 3A and B). It is presumed that the longer simulation time accounted for the higher negative binding free energy when compared with -33.54 kcal/mol reported in a previous study which only identified four interacting residues (ILE14, GLY94, PRO187, and VAL188) with OA at the active site of 17 β HSD1 (Kristanti et al., 2022). In the current study, as suggested by the literature (Frotscher et al.,

Table 3. MM/PBSA-based binding free energy thermodynamic analysis of Apo-OA and Apo-vincristine complexes (Mean \pm standard error of the mean).

Energy components (kcal/mol)	Apo-OA	Apo-Oestradiol	Apo-vincristine
ΔE_{vdw}	-58.28 ± 0.09	-37.57 ± 0.10	-77.41 ± 0.15
ΔE_{ele}	-9.88 ± 0.11	-17.50 ± 0.25	-138.26 ± 0.53
ΔG_{GB}	22.28 ± 0.10	22.24 ± 0.10	162.12 ± 0.54
ΔE_{surf}	-6.89 ± 0.01	-4.85 ± 0.01	-10.02 ± 0.01
ΔG_{gas}	-68.16 ± 0.13	-55.07 ± 0.26	-215.67 ± 0.54
ΔG_{solv}	15.39 ± 0.10	17.39 ± 0.10	152.11 ± 0.54
ΔG_{bind}	-52.76 ± 0.11	-37.68 ± 0.22	-63.56 ± 0.22

Table 2. Binding affinities (kcal/mol) of OA docked with nine cancer-related proteins.

Binding energy (kcal/mol)	1jff	1gfw	1fdw	1e8z	5ds3	7jkw	3ert	3fc2	5jeb
Proteins (PDB ID)									
Docking score	-8.3	-9.3	-9.8	-7.1	-8.9	-7.2	-6.9	-8.7	-9.1

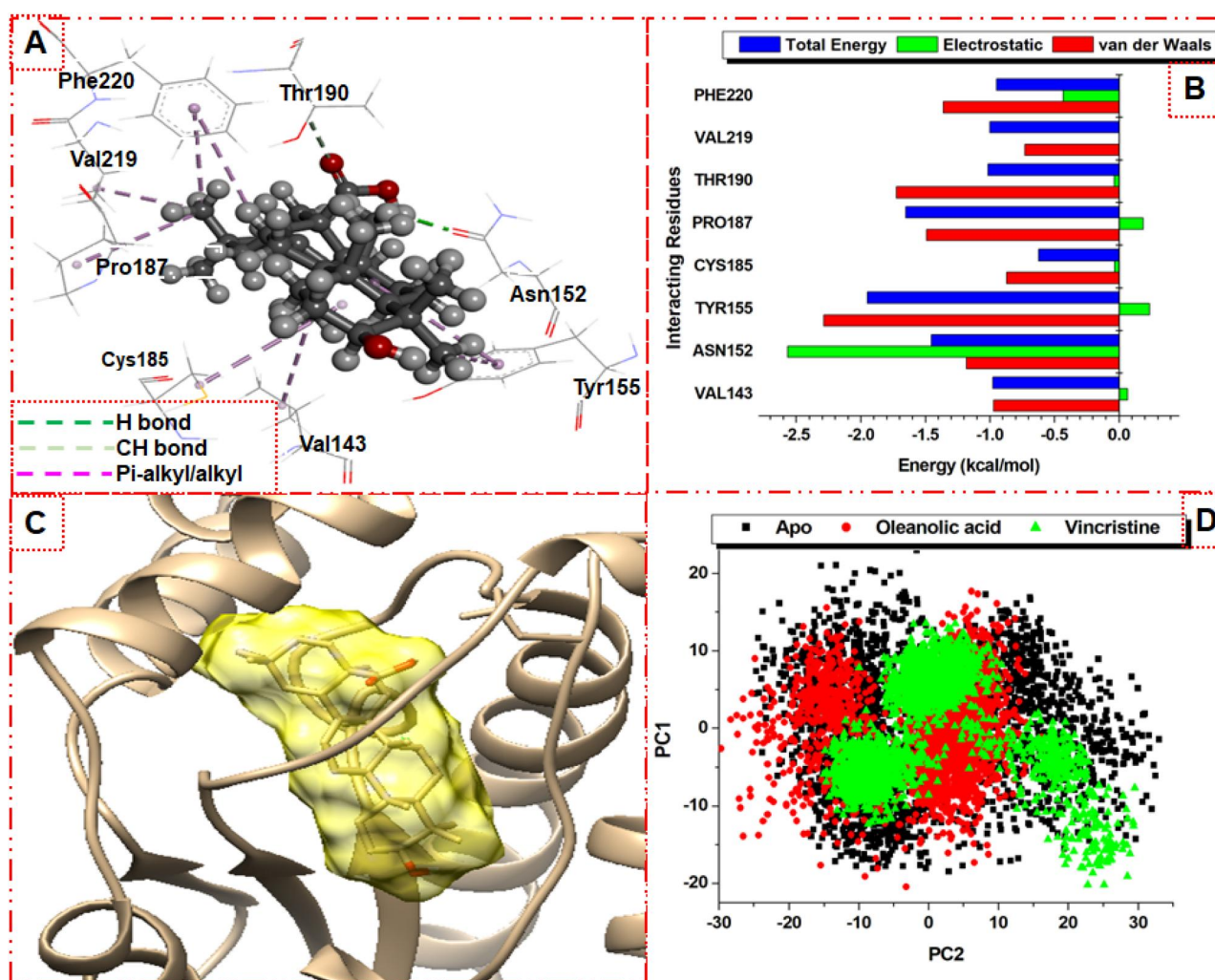


Figure 3. 3D structure (A), PRED (B), docked pose (C), and PCA (D) plots of OA against 17 β HSD1.

2008; Ghosh et al., 1995; Negri et al., 2010; Puranen et al., 1994), OA did interact with members of the 17 β HSD1 'catalytic triad' residues (TYR155) (Figure 3B) by π -alkyl interaction.

It has been reported that molecular docking or short MD simulations of receptor-ligand complexes do not produce stable complexes. Therefore, for a better result that reflects the inhibitory potential of such molecules, long-time MD simulations of the systems are carried out to enhance the stability of the conformations of such complexes (Adewumi et al., 2023). Hence, the MD studies for the most favourably proposed protein target (17 β HSD1) complexed with OA were carried out to validate the docking approach used in this study. The anticancer vinca alkaloid (vincristine) was used as the standard. The MD simulation was run for 240 ns. Visualisation of the amino acid residues participating in receptor-ligand interaction was carried out using BIOVIA Discovery Studio Visualizer 2021 client (Adewumi et al., 2023). The residue interaction of vincristine at the binding site of 17 β HSD1 shows hydrogen bonds with VAL143, THR192, ASN152 and TYR155 (Figure 3A). Also, vincristine shows pi-alkyl interaction with TYR155, and alkyl hydrophobic interactions with VAL143, LEU149 and CYS185. When simulated, OA's carbonyl group formed hydrogen bonding

with ASN152; pi-alkyl interactions with VAL143, TYR155, CYS185, PRO187, VAL219, and PHE220; and van der Waals interactions with ASN90, GLY92, LEU93, ASN114, THR140, GLY141, SER142, LYS159, GLY186, VAL188, and PHE253 (Figures 3A). TYR155 and LYS159 are involved in 17 β HSD1 enzyme catalysis (Puranen et al., 1994). Also, TYR155 is involved in the binding of a group of highly potent non-steroidal inhibitors (containing 2-benzylidenebenzofuran-3(2H)-one scaffold) of 17 β HSD1 to the enzyme (Starčević et al., 2011). In addition to the residues that constitute the "catalytic triad" (SER142, TYR155, LYS159), other residues such as VAL143 also showed interaction with flavonoid and cinnamic acid inhibitors of 17 β HSD1 (Brožič et al., 2009). Per-residue energy decomposition was also carried out to determine the contributions of interacting residues to the total binding free energy (Figure 3B). ASN152 contributed the highest electrostatic energy (-2.563 kcal/mol) to the binding energy of OA to 17 β HSD1. It has van der Waals energy of -1.181 kcal/mol and a total energy of -1.452 kcal/mol. TYR155 contributed the highest van der Waals force of -2.287 kcal/mol and the highest total energy of -1.950 kcal/mol. van der Waals interaction due to amino acid residues VAL143, ASN152, TYR155, CYS185, PRO187, THR190, VAL219, and PHE220 contributed the most to the -52.76 kcal/mol

energy of the OA-bound system (Figure 3B). The 17β -hydroxyl group of the co-crystallised ligand (oestradiol) stabilised with the receptor by hydrogen bonding with the TYR155 (He et al., 2016), a critical residue in the catalytic triad of 17β HSD1 (Negri et al., 2010; Puranen et al., 1994). Interacting with these catalytic amino acid residues (SER142, TYR155 and LYS159) suggests that OA might inhibit the catalytic functions of 17β HSD1, principally the bio-conversion of estrone to 17β -oestradiol (Ghosh et al., 1995). This peculiar interaction OA had with TYR155 is fundamental to the affinity and stabilisation of the inhibitor within the 17β HSD1 binding pocket. Since TYR155 is in the frontline in the 17β HSD1 catalysis (Puranen et al., 1994), it is plausible to suggest that the strongest individual energy of binding shown for van der Waals (-2.287 kcal/mol) and total energy (-1.950 kcal/mol) in the OA- 17β HSD1 bound system could contribute to the altering of the activity of 17β HSD1 in the catalytic conversion of oestrone to oestradiol in cancer pathogenesis. For the standard anticancer drug vincristine, VAL143 (-2.334 kcal/mol), TYR155 (-2.954 kcal/mol), and SER216 (-2.519 kcal/mol) represented the highest total energy contribution (Figure 4). In addition, GLU184 contributed a staggering -40.028 kcal/mol electrostatic energy.

3.4.2. RMSD, RMSF, and RoG

The C- α RMSD, RMSF, and RoG analyses are used to describe proteins conformational behaviours when ligands bind to

them during simulations. The structural organisation of a protein is a critical defining factor for its biological action, hence there could be either a positive or negative effect on the activities of such protein when there are considerable alterations in its structural integrity (Adewumi et al., 2023). RMSD defines the structural stability of Apo (17β HSD1) upon binding by OA and vincristine, thereby revealing the induced deviation of the C- α atom. A higher RMSD value indicates lower stability, while a lower value indicates higher stability. In Figure 5A, OA had a lower RMSD value (1.69 Å) when bound on 17β HSD1 relative to the unbound protein (2.01 Å), indicating a stable receptor-ligand complex. The results showed that all the simulated systems, except OA, displayed an average RMSD above 2 Å. By this, OA has demonstrated a more stable interaction with the active site residues of 17β HSD1. Likewise, all the simulated systems achieve convergence at approximately 40 ns up to the end of the simulation at 240 ns, except for the simulation time of around 150 to 165 ns which showed increased atomistic deviations (above 3 Å) in the Apo system relative to the bound systems. The significant reduction of the activity or the stabilisation of the structure of 17β HSD1 could be indicative of the inhibition of its enzymatic activity by OA (Olanlokun et al., 2019). It was observed that the OA-bound system achieved a more stabilising effect on the binding domain than vincristine (2.18 Å) and unbound conformations. The highly stable binding pocket residues observed in OA-bound could have favoured a steadier residue interaction with OA and possibly

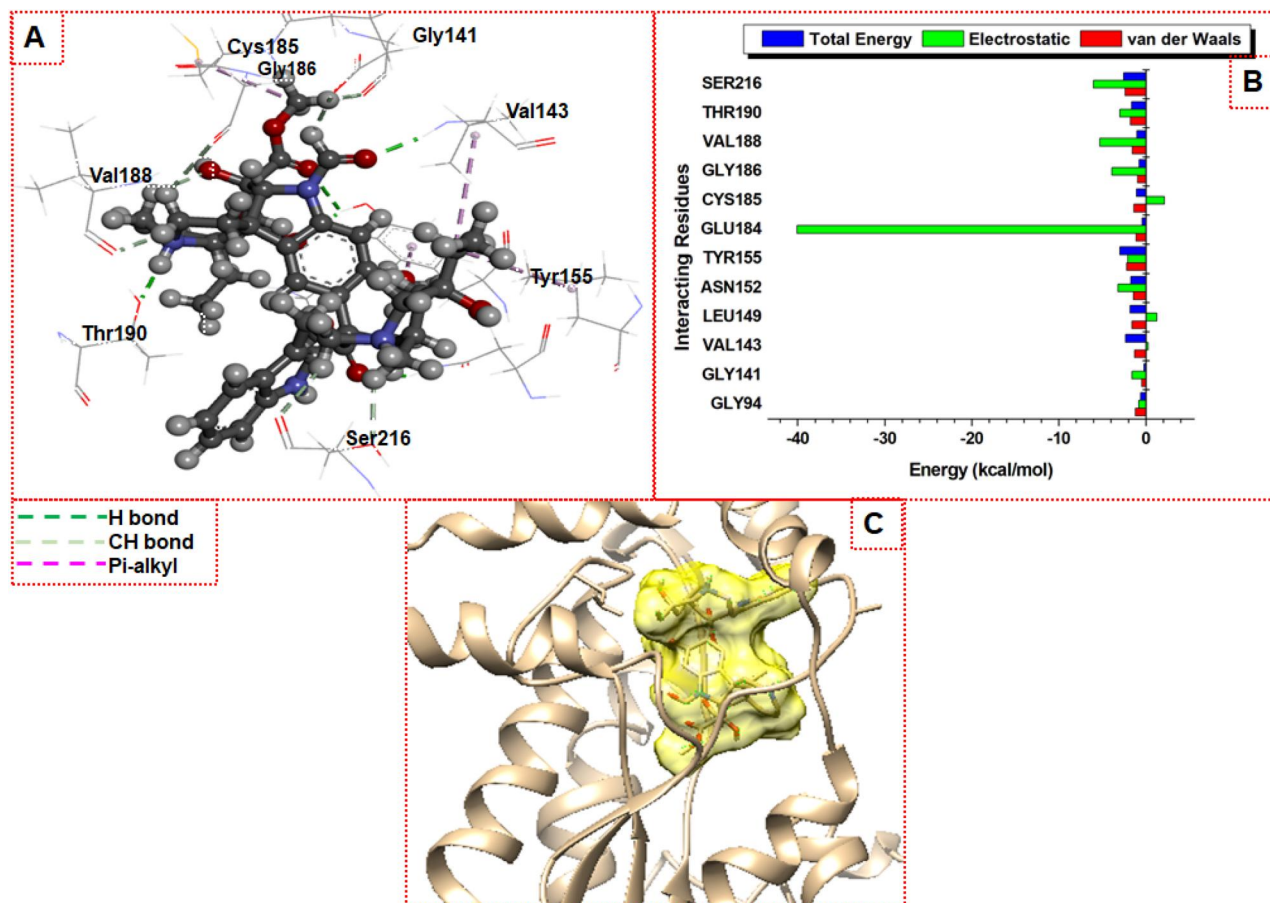


Figure 4. 3D structure (A) PRED (B), ligand-residue interaction network docked pose (C) of vincristine against 17β HSD1.

stronger binding to 17β HSD1 relative to vincristine. Unlike the current work, the study reported by Kristanti et al. (2022) did not show how the C- α RMSD value of the bound OA- 17β HSD1 system compared with that of the unbound Apo- 17β HSD1 system.

In addition, RMSF describes the residual flexibility upon binding by a ligand. It shows fluctuations in the protein residues during MD simulations. It gives an insight into the flexibility of various regions of proteins' residues when ligands bind to them (Adewumi et al., 2020). The differences in a protein's structural conformations before and after ligand binding can provide an understanding that helps in quantitatively measuring the induced functional or catalytic changes in the protein. A marked decreased flexibility of 17β HSD1 was observed upon OA binding (0.97 Å) compared with the unbound protein (1.22 Å) (Figure 5B). The results showed the flexibility of the protein's structure and the fluctuation of each amino acid residue present in the protein. The conformational changes of the active site residues play an important role in the overall function of the protein (Oluyemi et al., 2022). The higher RMSF values indicate more flexibility in the

protein's residue movement, while the lower fluctuation values show lesser conformational changes during the simulation. From the results, the unbound 17β HSD1 showed more residue fluctuation throughout the residue indices compared to the OA-bound system, except between residues 160–175 which are not part of the active site domain. By implication, the fluctuation of 17β HSD1 reduced upon the binding of OA. Moreover, the lower RMSF value of OA compared to the Apo system may indicate the system's compactness. This suggests that binding of OA to 17β HSD1 may alter the activities of the protein and its structural integrity thereby preventing the proliferation of breast cancer cells. Also, it is shown in the RMSF results some fluctuations above 3.0 Å. This occurrence is majorly noticed in the Apo structure around residues 192–197 and 265–268, indicating a more flexible movement of atoms within these domains compared to when OA and vincristine are binding. This suggests a lesser conformational change for OA- 17β HSD1 and vincristine- 17β HSD1 bound systems. The atomistic deviation seen in the RMSD results of the Apo system around the simulation time 150–165 ns (Figure A) corresponds with the high fluctuations observed

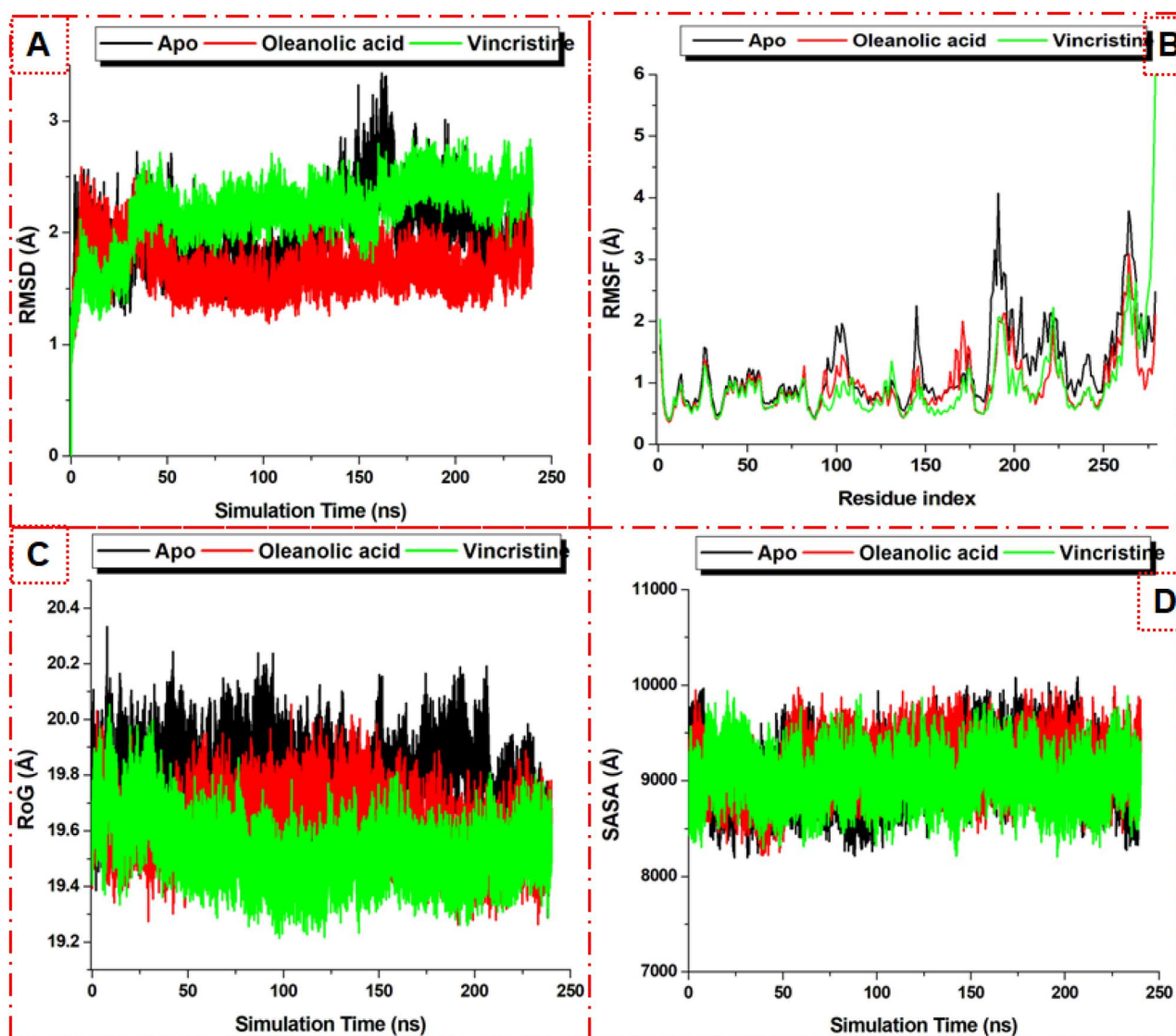


Figure 5. RMSD (A), RMSF (B), RoG (C), and SASA (D) plots of OA against 17β HSD1.

in the Apo system around residues 192–197 and 265–268 (Figure 5B). Assumably, it can be suggested that the atomistic deviations above 3.0 \AA that were observed in the Apo system of our RMSD experiment may be due to these highly fluctuated residues in the RMSF (Figure 5A and B). It should also be noted that these highly fluctuated residues are not within the active site domain, therefore, their activities may not directly impact the function of the protein when binding to the ligands. Furthermore, RoG measures the degree of structural compactness of a protein molecule bound to a ligand to further investigate the complexes' stability (Lobanov et al., 2008). The average RoG value of the OA-bound system (19.62 \AA) was lesser than that of unbound protein (19.79 \AA) and was comparable with that of the anticancer drug vincristine (19.53 \AA) (Figure 5C).

3.4.3. PCA and SASA

The principal component analysis (PCA) examines the magnitude (eigenvalues) and direction (eigenvectors) of a

protein's motion (Post et al., 2019). The first two components (PC1 and PC2) of the principal components analysis were calculated to determine the binding and interaction of OA. This is represented by the scatter plot in Figure 3D generated by the unbound $17\beta\text{HSD1}$ (black), OA- $17\beta\text{HSD1}$ (red), and vincristine- $17\beta\text{HSD1}$ (green). The C- α of $17\beta\text{HSD1}$ was more displaced along the eigenvectors compared with the C- α backbone of OA and vincristine (Figure 3D). In addition, solvent-accessible surface area (SASA) was calculated to further reveal the degree of alterations to the binding domain of $17\beta\text{HSD1}$ upon binding by OA. It shows the residues' mobility across the solvent region during the simulations. As seen in Figure 5D, the surface exposure of the residues lowered at 0–50 ns; and after this, the value increased slightly and only fluctuated around a constant value. Overall, the estimated average SASA values showed that the OA-bound system (9159.05 \AA^2) did not have a significantly different value compared with the unbound (9086.31 \AA^2). The insights from RMSD, RMSF, RoG, PCA, and SASA corroborate the binding free energy of OA, and it

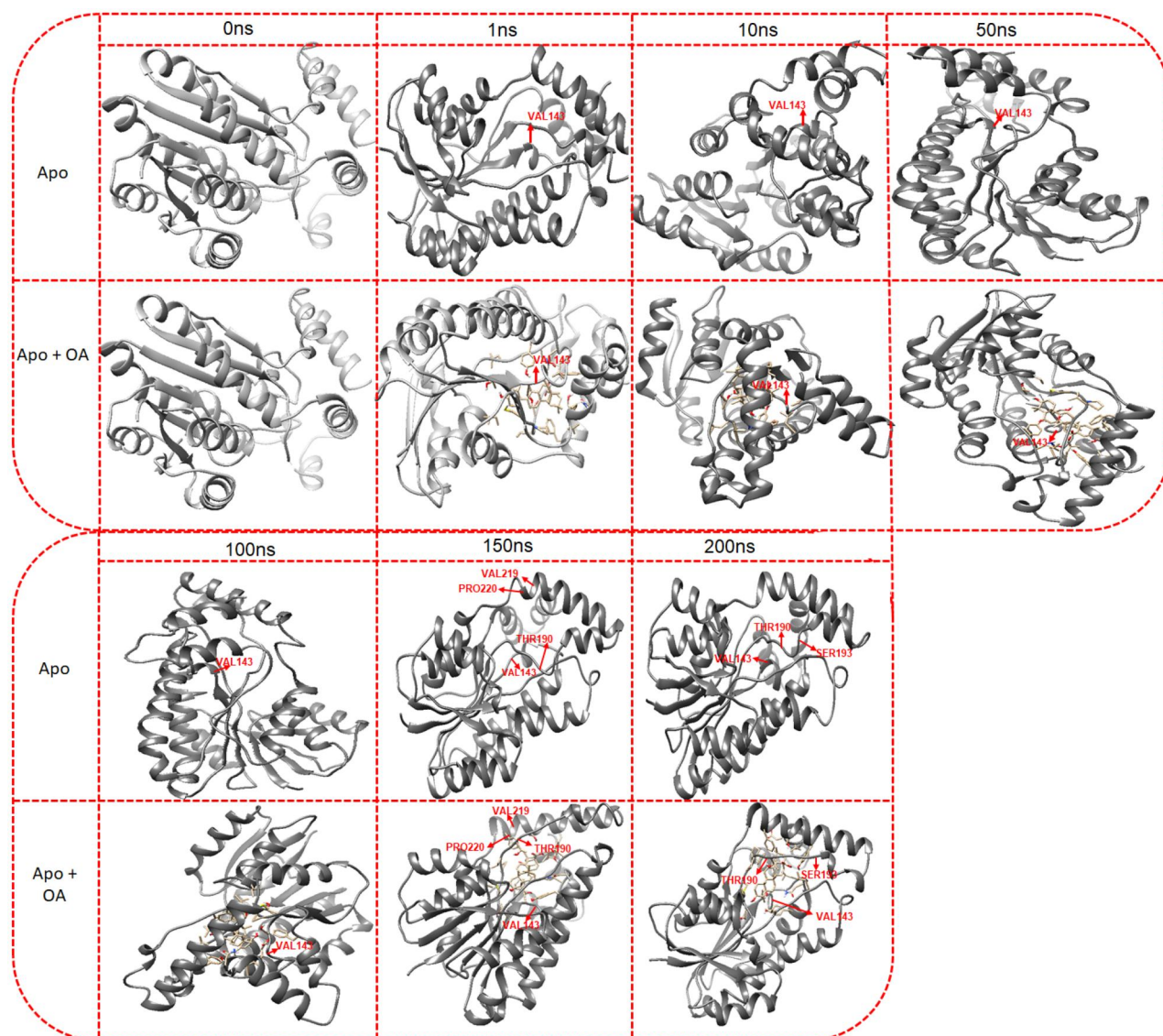


Figure 6. Trajectory snapshots showing structural changes to the active site residues between Apo and OA- $17\beta\text{HSD1}$ bound system at 0, 1, 10, 50, 100, 150 and 200 ns.

achieved conformation favouring the inhibition of the enzymatic activity of 17 β HSD1.

3.4.4. Structural dynamics of some critical residues at the active site of 17 β HSD1

The structures and dynamics of proteins are closely related to their functions and activities, and their interactions with ligands. Knowledge of the mechanistic events of proteins' conformational transitions and interactions with ligands is crucially important to understand the functions and biological activities of proteins and thus to the design of novel inhibitors of the targeted receptor (Li & Ji, 2019). We further investigated the possible conformational changes that occurred in the protein secondary structure in both Apo and Apo-OA bound systems at 0, 1, 10, 50, 100, 150 and 200 ns simulation time. This is an important study that shows modifications to the secondary structure of the protein as a result of ligand binding throughout simulations (Oluyemi et al., 2022). Structural and positional changes to the residues that are critical to the binding of OA were observed. Figure 6 shows some critical conformational changes in the structure of the protein. Various modifications were observed between the structures of Apo and ligand-bound system at different times. This study identified that the region bearing VAL143 (one of the critical residues involved in the binding of OA to 17 β HSD1) structurally transitioned from α -helix in the Apo to loop in the OA-bound system at 1 ns. The loop exhibited twisting at 100–200 ns. For the unbound system (Apo), VAL143 transitioned from the α -helix to loop at 150 ns and then moved back to the α -helix at 200 ns. The regions of 155–159 and 185–192 were in the α -helix throughout the simulation time. At 150 ns, the positions of the region bearing VAL219 and PRO220 changed between Apo and Apo-OA within the α -helix. Similarly, at 150 ns, a relaxation in the twisting of the loop region bearing THR190 was observed. The region of the loop bearing 190–193 was twisted in Apo at 200 ns, but the conformation of an untwisted loop was observed at the same time in the presence of the ligand (OA). The findings in this study indicate that OA could be a good scaffold for developing new anti-breast cancer drugs.

4. Conclusions

Inhibition of 17 β HSD1 is an attractive drug discovery target for hormone-dependent diseases such as breast cancer and endometriosis. This study reported the isolation and spectroscopic characterisation of oleanolic acid from the stem bark extract of *O. subscorpioidea* Oliv. The isolated compound was investigated for its binding affinity for nine cancer-related protein targets. MD trajectories were further calculated to gain insights into the inhibitory potential of OA on the substrate-binding site of 17 β HSD1. OA had binding free energy that is comparable with that of vincristine, and its average RMSD value indicated its high stability at the protein's active site. The binding energy and stability of OA at the active site of 17 β HSD1 indicated a profound inhibitory potential. This

study has demonstrated that OA could be a good scaffold for developing 17 β HSD1 inhibitors as anti-breast cancer agents. Since the cytotoxicity of OA discussed in the current study employed *in silico* models, further studies are recommended to experimentally validate 17 β HSD1 as the primary target responsible for the observed cytotoxic effects of OA. These may include specific enzymatic assays to evaluate the inhibitory effects of OA on 17 β HSD1, caspase-3, and EGFR activities in a cell-free system.

Acknowledgements

The authors acknowledge the Centre for High-Performance Computing, Cape Town, for providing computational resources.









Disclosure statement

No potential conflict of interest was reported by the authors.

Funding

Yemi Adekunle thanks the Government of the United Kingdom for the award of Commonwealth Split Site PhD Fellowship to visit Liverpool John Moores University for his PhD research (NGCN-2021-184). Lutfun Nahar gratefully acknowledges the financial support of the European Regional Development Fund – Project ENOCH (No. CZ.02.1.01/0.0/0.0/16_019/0000868) and the Czech Agency Grant – Project 23-05474S.

ORCID

Yemi A. Adekunle  <http://orcid.org/0000-0002-9392-3925>
 Babatunde B. Samuel  <http://orcid.org/0000-0001-5553-4438>
 Wande M. Oluyemi  <http://orcid.org/0000-0003-3646-2488>
 Adeniyi T. Adewumi  <http://orcid.org/0000-0002-7645-5517>
 Salerwe Mosebi  <http://orcid.org/0000-0002-7028-1712>
 Lutfun Nahar  <http://orcid.org/0000-0002-1157-2405>
 Amos A. Fatokun  <http://orcid.org/0000-0001-5183-7589>
 Satyajit D. Sarker  <http://orcid.org/0000-0003-4038-0514>

References

- Abdelrhheem, D. A., Rahman, A. A., Elsayed, K. N. M., Abd El-Mageed, H. R., Mohamed, H. S., & Ahmed, S. A. (2021). Isolation, characterization, *in vitro* anticancer activity, dft calculations, molecular docking, bioactivity score, drug-likeness and admet studies of eight phytoconstituents from brown alga sargassum platycarpum. *Journal of Molecular Structure*, 1225, 129245. <https://doi.org/10.1016/j.molstruc.2020.129245>
- Adekunle, Y. A., Samuel, B. B., Akinleye, T. E., Adeniji, A. J., & Ogbale, O. O. (2022). Cytotoxicity analysis of nineteen medicinal plants extracts on breast adeno-carcinoma (MCF-7) and rhabdomyosarcoma (RD) cancer cell lines. *Trends in Pharmaceutical Sciences*, 8(1), 57–64. <https://doi.org/10.30476/TIPS.2022.94313.1136>
- Adekunle, Y. A., Samuel, B. B., Fatokun, A. A., Nahar, L., & Sarker, S. D. (2022). *Olox subscorpioidea* Oliv. (Olacaceae): An ethnomedicinal and pharmacological review. *Journal of Natural Products Discovery*, 1(2), 1–15. <https://doi.org/10.24377/jnpd.article673>
- Adekunle, Y. A., Samuel, B. B., Nahar, L., Fatokun, A. A., & Sarker, S. D. (2023). Cytotoxic triterpenoid saponins from the root of *Olox subscorpioidea* Oliv. (Olacaceae). *Phytochemistry*, 215, 113853. <https://doi.org/10.1016/j.phytochem.2023.113853>
- Adewumi, A. T., Oluyemi, W. M., Adekunle, Y. A., Adewumi, N., Alahmdi, M. I., Soliman, M. E. S., & Abo-Dya, N. E. (2023). Propitious indazole compounds as β -ketoacyl-ACP synthase inhibitors and mechanisms unfolded

- for TB cure: Integrated rational design and MD simulations. *ChemistrySelect*, 8(3), e202203877. <https://doi.org/10.1002/slct.202203877>
- Adewumi, A. T., Soremekun, O. S., Ajadi, M. B., & Soliman, M. E. S. (2020). Thompson loop: Opportunities for antitubercular demethylmenaquinone methyltransferase protein. *RSC Advances*, 10(39), 23466–23483. <https://doi.org/10.1039/d0ra03206a>
- Agbabiaka, T. O., & Adebayo, I. A. (2021). The medicinal properties of *Olox subscorpioidea*. In R. A. Bhat, K. R. Hakeem, & M. A. Dervash (Eds.), *Phytomedicine: A Treasure of Pharmacologically Active Products from Plants* (pp. 555–580). Elsevier Inc. <https://doi.org/10.1016/b978-0-12-824109-7.00019-4>
- Ainsley, J., Lodola, A., Mulholland, A. J., Christov, C. Z., & Karabencheva-Christova, T. G. (2018). Combined quantum mechanics and molecular mechanics studies of enzymatic reaction mechanisms. In *Advances in protein chemistry and structural biology* (1st ed., Vol. 113, pp. 1–32). Elsevier Inc. <https://doi.org/10.1016/bs.apcsb.2018.07.001>
- Aka, J. A., Mazumdar, M., Chen, C. Q., Poirier, D., & Lin, S. X. (2010). 17 β -Hydroxysteroid dehydrogenase type 1 stimulates breast cancer by dihydrotestosterone inactivation in addition to estradiol production. *Molecular Endocrinology*, 24(4), 832–845. <https://doi.org/10.1210/me.2009-0468>
- Aouane, C., Kabouche, A., Voutquenne-Nazabadioko, L., Sayagh, C., Martinez, A., Alabdul Magid, A., & Kabouche, Z. (2022). Triterpenoid saponins from *Anagallis monelli* ssp. *linifolia* (L.) Maire and their chemotaxonomic significance. *Phytochemistry*, 202, 113305. <https://doi.org/10.1016/j.phytochem.2022.113305>
- Ayan, D., Maltais, R., Roy, J., & Poirier, D. (2012). A new nonsteroidal inhibitor of 17 β -hydroxysteroid dehydrogenase type I blocks the estrogen-dependent breast cancer tumor growth induced by estrone. *Molecular Cancer Therapeutics*, 11(10), 2096–2104. <https://doi.org/10.1158/1535-7163.MCT-12-0299>
- Azzi, A., Rehse, P. H., Zhu, D.-W., Campbell, R. L., Labrie, F., & Lin, S.-X. (1996). Crystal structure of human estrogenic 17 β -hydroxysteroid dehydrogenase complexed with 17 β -estradiol. *Nature Structural Biology*, 3(8), 665–668. <https://doi.org/10.1038/nsb0896-665>
- Berendsen, H. J. C., Postma, J. P. M., Van Gunsteren, W. F., Dinola, A., & Haak, J. R. (1984). Molecular dynamics with coupling to an external bath. *The Journal of Chemical Physics*, 81(8), 3684–3690. <https://doi.org/10.1063/1.448118>
- Berman, H. M., Westbrook, J., Feng, Z., Gilliland, G., Bhat, T. N., Weissig, H., Shindyalov, I. N., & Bourne, P. E. (2000). The Protein Data Bank. *Nucleic Acids Research*, 28(1), 235–242. <https://doi.org/10.1093/nar/28.1.235>
- Brožič, P., Kocbek, P., Sova, M., Kristl, J., Martens, S., Adamski, J., Gobec, S., & Lanisnik Rizner, T. (2009). Flavonoids and cinnamic acid derivatives as inhibitors of 17 β -hydroxysteroid dehydrogenase type 1. *Molecular and Cellular Endocrinology*, 301(1-2), 229–234. <https://doi.org/10.1016/j.mce.2008.09.004>
- Case, D. A., Walker, R. C., Cheatham, T. E., Simmerling, C., Roitberg, A., Merz, K. M., Luo, R., Darden, T. W., Wang, J., Duke, R. E., Roe, D. R., LeGrand, S., Swails, J., Götz, A. W., Smith, J., Cerutti, D., Brozell, S. R., Luchko, T., Cruzeiro, V. W. D., ... Kollman, P. A. (2018). *Amber 2018*. University of California. <http://ambermd.org/doc12/Amber18.pdf>
- Dawicki-McKenna, J. M., Langelier, M. F., DeNizio, J. E., Riccio, A. A., Cao, C. D., Karch, K. R., McCauley, M., Steffen, J. D., Black, B. E., & Pascal, J. M. (2015). PARP-1 activation requires local unfolding of an autoinhibitory domain. *Molecular Cell*, 60(5), 755–768. <https://doi.org/10.1016/j.molcel.2015.10.013>
- Day, J. M., Foster, P. A., Tutill, H. J., Parsons, M. F. C., Newman, S. P., Chander, S. K., Allan, G. M., Lawrence, H. R., Vicker, N., Potter, B. V. L., Reed, M. J., & Purohit, A. (2008). 17 β -Hydroxysteroid dehydrogenase Type 1, and not Type 12, is a target for endocrine therapy of hormone-dependent breast cancer. *International Journal of Cancer*, 122(9), 1931–1940. <https://doi.org/10.1002/ijc.23350>
- Dong, Y. W., Liao, M. L., Meng, X. L., & Somero, G. N. (2018). Structural flexibility and protein adaptation to temperature: Molecular dynamics analysis of malate dehydrogenases of marine molluscs. *Proceedings of the National Academy of Sciences of the United States of America*, 115(6), 1274–1279. <https://doi.org/10.1073/pnas.1718910115>
- Feng, J.-H., Chen, W., Zhao, Y., & Ju, X.-L. (2009). Anti-tumor activity of oleanolic, ursolic and glycyrrhetic acid. *The Open Natural Products Journal*, 2(1), 48–52. <https://doi.org/10.2174/1874848100902010048>
- Forgacs, P., & Provost, J. (1981). Oloxoside, a saponin from *Olox androsensis*, *Olox glabriflora* and *Olox psittacorum*. *Phytochemistry*, 20(7), 1689–1691. [https://doi.org/10.1016/S0031-9422\(00\)98556-X](https://doi.org/10.1016/S0031-9422(00)98556-X)
- Frotscher, M., Ziegler, E., Marchais-Oberwinkler, S., Kruchten, P., Neugebauer, A., Fetzer, L., Scherer, C., Müller-Vieira, U., Messinger, J., Thole, H., & Hartmann, R. W. (2008). Design, synthesis, and biological evaluation of (hydroxyphenyl)naphthalene and -quinoline derivatives: Potent and selective nonsteroidal inhibitors of 17 β -hydroxysteroid dehydrogenase type 1 (17 β -HSD1) for the treatment of estrogen-dependent diseases. *Journal of Medicinal Chemistry*, 51(7), 2158–2169. <https://doi.org/10.1021/jm701447v>
- Gbadamosi, I. T., & Erinoso, S. M. (2016). A review of twenty ethnobotanicals used in the management of breast cancer in Abeokuta, Ogun State, Nigeria. *African Journal of Pharmacy and Pharmacology*, 10(27), 546–564. <https://doi.org/10.5897/AJPP2015.4327>
- Ghosh, D., Pletnev, V. Z., Zhu, D. W., Wawrzak, Z., Duax, W. L., Pangborn, W., Labrie, F., & Lin, S. X. (1995). Structure of human estrogenic 17 β -hydroxysteroid dehydrogenase at 2.20 Å resolution. *Structure*, 3(5), 503–513. [https://doi.org/10.1016/S0969-2126\(01\)00183-6](https://doi.org/10.1016/S0969-2126(01)00183-6)
- Gyanani, V., Haley, J. C., & Goswami, R. (2021). Challenges of current anti-cancer treatment approaches with focus on liposomal drug delivery systems. *Pharmaceuticals*, 14(9), 835. <https://doi.org/10.3390/ph14090835>
- Harrach, M. F., & Drossel, B. (2014). Structure and dynamics of TIP3P, TIP4P, and TIP5P water near smooth and atomistic walls of different hydroaffinity. *The Journal of Chemical Physics*, 140(17), 174501. <https://doi.org/10.1063/1.4872239>
- He, W., Gauri, M., Li, T., Wang, R., & Lin, S.-X. (2016). Current knowledge of the multifunctional 17 β -hydroxysteroid dehydrogenase type 1 (HSD17B1). *Gene*, 588(1), 54–61. <https://doi.org/10.1016/j.gene.2016.04.031>
- Hollingsworth, S. A., & Dror, R. O. (2018). Molecular dynamics simulation for all. *Neuron*, 99(6), 1129–1143. <https://doi.org/10.1016/j.neuron.2018.08.011>
- Hsu, H.-F., Houg, J.-Y., Chang, C.-L., Wu, C.-C., Chang, F.-R., & Wu, Y.-C. (2005). Antioxidant activity, cytotoxicity, and DNA information of *Glossogyne tenuifolia*. *Journal of Agricultural and Food Chemistry*, 53(15), 6117–6125. <https://doi.org/10.1021/jf050463u>
- Huang, K., Fang, W., Li, A. F., Liang, P., Wu, C., Shyr, Y.-M., & Yang, M.-H. (2018). Caspase-3, a key apoptotic protein, as a prognostic marker in gastric cancer after curative surgery. *International Journal of Surgery (London, England)*, 52(March), 258–263. <https://doi.org/10.1016/j.ijsu.2018.02.055>
- Kipre, G. R., Akakpo-Akué, M., Brice Bla, K., & Djaman, A. J. (2015). Assessment of the combined action of chloroquine and *Olox subscorpioidea* on *Plasmodium falciparum* strains resistant in vitro culture. *International Journal of Innovation and Applied Studies*, 11(4), 947–952. <http://www.ijias.issr-journals.org/>
- Kristanti, A. N., Aminah, N. S., Siswanto, I., Manuhara, Y. S. W., Abdjan, M. I., Wardana, A. P., Aung, E. E., & Takaya, Y. (2022). Anticancer potential of β -sitosterol and oleanolic acid as through inhibition of human estrogenic 17 β -hydroxysteroid dehydrogenase type-1 based on an in silico approach. *RSC Advances*, 12(31), 20319–20329. <https://doi.org/10.1039/d2ra03092f>
- Lee, D., Long, S. A., Adams, J. L., Chan, G., Vaidya, K. S., Francis, T. A., Kikly, K., Winkler, J. D., Sung, C. M., Debouck, C., Richardson, S., Levy, M. A., DeWolf, W. E., Keller, P. M., Tomaszek, T., Head, M. S., Ryan, M. D., Haliwanger, R. C., Liang, P. H., ... Nuttall, M. E. (2000). Potent and selective nonpeptide inhibitors of caspases 3 and 7 inhibit apoptosis and maintain cell functionality. *The Journal of Biological Chemistry*, 275(21), 16007–16014. <https://doi.org/10.1074/jbc.275.21.16007>
- Lee, T.-S., Hu, Y., Sherborne, B., Guo, Z., & York, D. M. (2017). Toward fast and accurate binding affinity prediction with pmemdGTI: An efficient implementation of GPU-accelerated thermodynamic integration. *Journal of Chemical Theory and Computation*, 13(7), 3077–3084. <https://doi.org/10.1021/acs.jctc.7b00102>
- Li, D., & Ji, B. (2019). Protein conformational transitions coupling with ligand interactions: Simulations from molecules to medicine. *Medicine in Novel*

- Technology and Devices*, 3, 100026. <https://doi.org/10.1016/j.medntd.2019.100026>
- Li, Y., Zhao, J., Gutgesell, L. M., Shen, Z., Ratia, K., Dye, K., Dubrovskiy, O., Zhao, H., Huang, F., Tonetti, D. A., Thatcher, G. R. J., & Xiong, R. (2020). Novel pyrrolopyridone bromodomain and extra-terminal motif (BET) inhibitors effective in endocrine-resistant ER+ breast cancer with acquired resistance to fulvestrant and palbociclib. *Journal of Medicinal Chemistry*, 63(13), 7186–7210. <https://doi.org/10.1021/acs.jmedchem.0c00456>
- Lilienkamp, A., Karkola, S., Alho-Richmond, S., Koskimies, P., Johansson, N., Huhtinen, K., Vihko, K., & Wähälä, K. (2009). Synthesis and biological evaluation of 17 β -hydroxysteroid dehydrogenase type 1 (17 β -HSD1) inhibitors based on a thieno[2,3-d] pyrimidin-4(3H)-one core. *Journal of Medicinal Chemistry*, 52(21), 6660–6671. <https://doi.org/10.1021/jm900928k>
- Lobanov, M. Y., Bogatyreva, N. S., & Galzitskaya, O. V. (2008). Radius of gyration as an indicator of protein structure compactness. *Molecular Biology*, 42(4), 623–628. <https://doi.org/10.1134/S0026893308040195>
- Löwe, J., Li, H., Downing, K. H., & Nogales, E. (2001). Refined structure of $\alpha\beta$ -tubulin at 3.5 Å resolution. *Journal of Molecular Biology*, 313(5), 1045–1057. <https://doi.org/10.1006/jmbi.2001.5077>
- Mahato, S. B., & Kundu, A. P. (1994). ¹³C NMR spectra of pentacyclic triterpenoids—a compilation and some salient features. *Phytochemistry*, 37(6), 1517–1575. [https://doi.org/10.1016/S0031-9422\(00\)89569-2](https://doi.org/10.1016/S0031-9422(00)89569-2)
- Mazza, C., Breton, R., Housset, D., & Fontecilla-Camps, J. C. (1998). Unusual charge stabilization of NADP+ in 17 β -hydroxysteroid dehydrogenase. *The Journal of Biological Chemistry*, 273(14), 8145–8152. <https://doi.org/10.1074/jbc.273.14.8145>
- Mosmann, T. (1983). Rapid colorimetric assay for cellular growth and survival: Application to proliferation and cytotoxicity assays. *Journal of Immunological Methods*, 65(1-2), 55–63. <https://doi.org/10.1039/c6ra17788c>
- Moumbock, A. F. A., Li, J., Mishra, P., Gao, M., & Günther, S. (2019). Current computational methods for predicting protein interactions of natural products. *Computational and Structural Biotechnology Journal*, 17, 1367–1376. <https://doi.org/10.1016/j.csbj.2019.08.008>
- Mucs, D., & Bryce, R. A. (2013). The application of quantum mechanics in structure-based drug design. *Expert Opinion on Drug Discovery*, 8(3), 263–276. <https://doi.org/10.1517/17460441.2013.752812>
- Nazifi, A. B., Saidi, O., & Ismail, H. F. (2015). Evaluation of anticonvulsant effects of methanolic extract of *Olax subscorpioidea* Oliv. leaves in chicks and mice. *Journal of Pharmacy & Bioresources*, 12(2), 165. <https://doi.org/10.4314/jpb.v12i2.12>
- Negri, M., Recanatini, M., & Hartmann, R. W. (2010). Insights in 17 β -HSD1 enzyme kinetics and ligand binding by dynamic motion investigation. *PLoS One*, 5(8), e12026. <https://doi.org/10.1371/journal.pone.0012026>
- Newman, D. J., & Cragg, G. M. (2020). Natural products as sources of new drugs over the nearly four decades from 01/1981 to 09/2019. *Journal of Natural Products*, 83(3), 770–803. <https://doi.org/10.1021/acs.jnatprod.9b01285>
- Nguyen, H. T. M., Vo, N. T., Huynh, S. T. M., Do, L. T. M., Aree, T., Tip-Pyang, S., Phan, C. T. D., Trung, N. T., & Nguyen, P. K. P. (2019). A sesquiterpenoid tropolone and 1,2,3,4-tetrahydronaphthalene derivatives from *Olax imbricata* roots. *Fitoterapia*, 132(September 2018), 1–6. <https://doi.org/10.1016/j.fitote.2018.11.007>
- Niinivehmas, S., Postila, P. A., Rauhamäki, S., Manivannan, E., Kortet, S., Ahinko, M., Huuskonen, P., Nyberg, N., Koskimies, P., Lätti, S., Multamäki, E., Juvonen, R. O., Raunio, H., Pasanen, M., Huuskonen, J., & Pentikäinen, O. T. (2018). Blocking oestradiol synthesis pathways with potent and selective coumarin derivatives. *Journal of Enzyme Inhibition and Medicinal Chemistry*, 33(1), 743–754. <https://doi.org/10.1080/14756366.2018.1452919>
- Novotny, C. J., Pollari, S., Park, J. H., Lemmon, M. A., Shen, W., & Shokat, K. M. (2016). Overcoming resistance to HER2 inhibitors through state-specific kinase binding. *Nature Chemical Biology*, 12(11), 923–930. <https://doi.org/10.1038/nchembio.2171>
- Okoye, F. B. C., Ngwoke, K. G., Debbab, A., Osadebe, P. O., & Proksch, P. (2016). Olamannosides D and E: Further kaempferol triglycosides from *Olax mannii* leaves. *Phytochemistry Letters*, 16, 152–155. <https://doi.org/10.1016/j.phytol.2016.04.006>
- Okoye, F. B. C., Sawadogo, W. R., Sendker, J., Aly, A. H., Quandt, B., Wray, V., Hensel, A., Esimone, C. O., Debbab, A., Diederich, M., & Proksch, P. (2015). Flavonoid glycosides from *Olax mannii*: Structure elucidation and effect on the nuclear factor kappa B pathway. *Journal of Ethnopharmacology*, 176, 27–34. <https://doi.org/10.1016/j.jep.2015.10.019>
- Olabanji, S. O., Adebajo, A. C., Omobuwajo, O. R., Ceccato, D., Buoso, M. C., & Moschini, G. (2014). PIXE analysis of some Nigerian anti-diabetic medicinal plants (II). *Nuclear Instruments and Methods in Physics Research Section B: Beam Interactions with Materials and Atoms*, 318, 187–190. <https://doi.org/10.1016/j.nimb.2013.06.052>
- Oladipo, S. D., Luckay, R. C., Olofinisan, K. A., Obakachi, V. A., Zamisa, S. J., Adeleke, A. A., Badeji, A. A., Ogundare, S. A., & George, B. P. (2024). Antidiabetes and antioxidant potential of Schiff bases derived from 2-naphthaldehyde and substituted aromatic amines: Synthesis, crystal structure, Hirshfeld surface analysis, computational, and invitro studies. *Heliyon*, 10(1), e23174. <https://doi.org/10.1016/j.heliyon.2023.e23174>
- Oladipupo, A. R., Alaribe, S. C. A., Ogunlaja, A. S., Beniddir, M. A., Gordon, A. T., Ogah, C. O., Okpuzor, J., & Coker, H. A. B. (2023). Structure-based molecular networking, molecular docking, dynamics simulation and pharmacokinetic studies of *Olax subscorpioidea* for identification of potential inhibitors against selected cancer targets. *Journal of Biomolecular Structure & Dynamics*, 42(3), 1110–1125. <https://doi.org/10.1080/07391102.2023.2198032>
- Olanlokun, J. O., Olotu, A. F., David, O. M., Idowu, T. O., Soliman, E. S. M., & Olorunsogo, O. O. (2019). A novel compound purified from *Alstonia boonei* inhibits Plasmodium falciparum lactate dehydrogenase and plasmeprin II. *Journal of Biomolecular Structure & Dynamics*, 37(8), 2193–2200. <https://doi.org/10.1080/07391102.2018.1483840>
- Olowokudejo, J., Kadiri, A., & Travih, V. (2008). An ethnobotanical survey of herbal markets and medicinal plants in Lagos state of Nigeria. *Ethnobotanical Leaflets*, 12, 851–865.
- Oluyemi, W. M., Samuel, B. B., Adewumi, A. T., Adekunle, Y. A., Soliman, M. E. S., & Krenn, L. (2022). An allosteric inhibitory potential of triterpenes from *Combretum racemosum* on the structural and functional dynamics of Plasmodium falciparum lactate dehydrogenase binding landscape. *Chemistry & Biodiversity*, 19(2), e202100646. <https://doi.org/10.1002/cbdv.202100646>
- Parikh, N. R., Mandal, A., Bhatia, D., Siveen, K. S., Sethi, G., & Bishayee, A. (2014). Oleanane triterpenoids in the prevention and therapy of breast cancer: Current evidence and future perspectives. *Phytochemistry Reviews*, 13(4), 793–810. <https://doi.org/10.1007/s11101-014-9337-5>
- Pertuit, D., Mitaine-Offer, A. C., Miyamoto, T., Tanaka, C., Delaude, C., & Lacaille-Dubois, M. A. (2018). Triterpene saponins of the root bark of *Olax obtusifolia* De Wild. *Phytochemistry Letters*, 28(September), 174–178. <https://doi.org/10.1016/j.phytol.2018.09.018>
- Pettersen, E. F., Goddard, T. D., Huang, C. C., Couch, G. S., Greenblatt, D. M., Meng, E. C., & Ferrin, T. E. (2004). UCSF Chimera – A visualization system for exploratory research and analysis. *Journal of Computational Chemistry*, 25(13), 1605–1612. <https://doi.org/10.1002/jcc.20084>
- Poirier, D., Nyachio, A., Romano, A., Roy, J., Maltais, R., Chai, D., Delvoux, B., Tomassetti, C., & Vanhie, A. (2022). An irreversible inhibitor of 17 β -hydroxysteroid dehydrogenase type 1 inhibits estradiol synthesis in human endometriosis lesions and induces regression of the non-human primate endometriosis. *The Journal of Steroid Biochemistry and Molecular Biology*, 222, 106136. <https://doi.org/10.1016/j.jsbmb.2022.106136>
- Post, M., Wolf, S., & Stock, G. (2019). Principal component analysis of nonequilibrium molecular dynamics simulations. *The Journal of Chemical Physics*, 150(20), 204110. <https://doi.org/10.1063/1.5089636>
- Puranen, T. J., Poutanen, M. H., Peltoketo, H. E., Vihko, P. T., & Vihko, R. K. (1994). Site-directed mutagenesis of the putative active site of human 17 β -hydroxysteroid dehydrogenase type 1. *The Biochemical Journal*, 304(Pt 1), 289–293. <https://doi.org/10.1042/bj3040289>
- Rasheed, H. M., Farooq, U., Bashir, K., Wahid, F., Khan, T., Khusro, A., Gajdács, M., Alghamdi, S., Alsaari, A. A., Almeahmadi, M., Afzal, S., & Sahibzada, M. U. K. (2023). Isolation of oleanolic acid from *Lavandula stoechas* and its potent anticancer properties against MCF-7 cancer cells via induced apoptosis. *Journal of King Saud University – Science*, 35(2), 102454. <https://doi.org/10.1016/j.jksus.2022.102454>

- Rathod, S., Shinde, K., Porlekar, J., Choudhari, P., Dhavale, R., Mahuli, D., Tamboli, Y., Bhatia, M., Haval, K. P., Al-Sehemi, A. G., & Pannipara, M. (2023). Computational exploration of anti-cancer potential of flavonoids against cyclin-dependent kinase 8: An in silico molecular docking and dynamic approach. *ACS Omega*, 8(1), 391–409. <https://doi.org/10.1021/acsomega.2c04837>
- Rižner, T. L., & Romano, A. (2023). Targeting the formation of estrogens for treatment of hormone dependent diseases—current status. *Frontiers in Pharmacology*, 14, 1155558. <https://doi.org/10.3389/fphar.2023.1155558>
- Roe, D. R., & Cheatham, T. E. (2013). PTRAJ and CPPTRAJ: Software for processing and analysis of molecular dynamics trajectory data. *Journal of Chemical Theory and Computation*, 9(7), 3084–3095. <https://doi.org/10.1021/ct400341p>
- Rudolph, D., Steegmaier, M., Hoffmann, M., Grauert, M., Baum, A., Quant, J., Haslinger, C., Garin-Chesa, P., & Adolf, G. R. (2009). BI 6727, a polo-like kinase inhibitor with improved pharmacokinetic profile and broad antitumor activity. *Clinical Cancer Research*, 15(9), 3094–3102. <https://doi.org/10.1158/1078-0432.CCR-08-2445>
- Sarker, S. D., Nahar, L., Miron, A., & Guo, M. (2020). Anticancer natural products. In *Annual Reports in Medicinal Chemistry* (Vol. 55, pp. 45–75). Elsevier. <https://doi.org/10.1016/bs.armc.2020.02.001>
- Seebacher, W., Simic, N., Weis, R., Saf, R., & Kunert, O. (2003). Complete assignments of ¹H and ¹³C NMR resonances of oleanolic acid, 18 α -oleanolic acid, ursolic acid and their 11-oxo derivatives. *Magnetic Resonance in Chemistry*, 41(8), 636–638. <https://doi.org/10.1002/mrc.1214>
- Shiau, A. K., Barstad, D., Loria, P. M., Cheng, L., Kushner, P. J., Agard, D. A., & Greene, G. L. (1998). The structural basis of estrogen receptor/coactivator recognition and the antagonism of this interaction by tamoxifen. *Cell*, 95(7), 927–937. [https://doi.org/10.1016/S0092-8674\(00\)81717-1](https://doi.org/10.1016/S0092-8674(00)81717-1)
- Soladoye, M. O., Amusa, N. A., Raji-Esan, S. O., Chukwuma, E. C., & Taiwo, A. A. (2010). Ethnobotanical survey of anti-cancer plants in Ogun State, Nigeria. *Annals of Biological Research*, 1(4), 261–273.
- Starčević, Š., Turk, S., Brus, B., Cesar, J., Lanišnik Rižner, T., & Gobec, S. (2011). Discovery of highly potent, nonsteroidal 17 β -hydroxysteroid dehydrogenase type 1 inhibitors by virtual high-throughput screening. *The Journal of Steroid Biochemistry and Molecular Biology*, 127(3–5), 255–261. <https://doi.org/10.1016/j.jsbmb.2011.08.013>
- Sule, M. I., Hassan, H., Pateh, U., & Ambi, A. (2011). Triterpenoids from the leaves of *Olax mannii*. *Nigerian Journal of Basic and Applied Science*, 19(2), 193–196.
- Sung, H., Ferlay, J., Siegel, R. L., Laversanne, M., Soerjomataram, I., Jemal, A., & Bray, F. (2021). Global Cancer Statistics 2020: GLOBOCAN estimates of incidence and mortality worldwide for 36 cancers in 185 countries. *CA: A Cancer Journal for Clinicians*, 71(3), 209–249. <https://doi.org/10.3322/caac.21660>
- Thomsen, R., & Christensen, M. H. (2006). MolDock: A new technique for high-accuracy molecular docking. *Journal of Medicinal Chemistry*, 49(11), 3315–3321. <https://doi.org/10.1021/jm051197e>
- Tripathi, A., & Bankaitis, V. A. (2017). Molecular docking: From lock and key to combination lock. *Journal of Molecular Medicine and Clinical Applications*, 2(1), 1–19. <https://doi.org/10.16966/2575-0305.106>
- Trott, O., & Olson, A. J. (2010). AutoDock Vina: Improving the speed and accuracy of docking with a new scoring function, efficient optimization, and multithreading. *Journal of Computational Chemistry*, 31(2), 455–461. <https://doi.org/10.1002/jcc.21334>
- Tsakem, B., Ponou, K. B., Toussie, B. T., Tematio, R. F., Noundou, X. S., Krause, R. W. M., Teponno, R. B., & Tapondjou, L. A. (2022). Natural products chemistry of botanical medicines from Cameroonian plants. In X. Siwe-Noundou & R. Cooper (Eds.), *Natural products chemistry of global plants* (1st ed., pp. 1–20). Taylor & Francis Group CRS Press. <https://doi.org/10.1201/9780429506734>
- Tsakem, B., Tchuenguem, R. T., Siwe-Noundou, X., Kemvoufo, B. P., Dzoyem, J. P., Teponno, R. B., Krause, R. W. M., & Tapondjou, L. A. (2023). New bioactive flavonoid glycosides with antioxidant activity from the stem bark of *Olax subscorpioidea* Oliv. *Natural Product Research*, 37(10), 1641–1650. <https://doi.org/10.1080/14786419.2022.2106566>
- Tsakem, B., Toussie, B. T., Siwe-Noundou, X., Ponou, B. K., Teponno, R. B., Musharraf, S. G., & Tapondjou, L. A. (2023). Structure elucidation of olasubscorpioside C, a new rotameric biflavonoid glycoside from the stem barks of *Olax subscorpioidea* (Oliv). *Magnetic Resonance in Chemistry*, 61(8), 497–503. <https://doi.org/10.1002/mrc.5375>
- Uribe, M. L., Marrocco, I., & Yarden, Y. (2021). EGFR in cancer: Signaling mechanisms, drugs, and acquired resistance. *Cancers*, 13(11), 2748. <https://doi.org/10.3390/cancers13112748>
- Vo, N. T., Minh Huynh, S. T., My Nguyen, H. T., Duong, H. T., & Nguyen, P. K. P. (2019). Triterpenoid glycosides from *Olax imbricata*. *Science and Technology Development Journal*, 22(3), 324–334. <https://doi.org/10.32508/stdj.v22i3.1660>
- Walker, E. H., Pacold, M. E., Perisic, O., Stephens, L., Hawkins, P. T., Wymann, M. P., & Williams, R. L. (2000). Structural determinants of phosphoinositide 3-kinase inhibition by wortmannin, LY294002, quercetin, myricetin, and staurosporine. *Molecular Cell*, 6(4), 909–919. [https://doi.org/10.1016/S1097-2765\(05\)00089-4](https://doi.org/10.1016/S1097-2765(05)00089-4)
- Wang, E., Sun, H., Wang, J., Wang, Z., Liu, H., Zhang, J. Z. H., & Hou, T. (2019). End-point binding free energy calculation with MM/PBSA and MM/GBSA: Strategies and applications in drug design. *Chemical Reviews*, 119(16), 9478–9508. <https://doi.org/10.1021/acs.chemrev.9b00055>
- Weinberg, F., Peckys, D. B., & Jonge, N. D. (2020). EGFR expression in HER2-driven Breast cancer cells. *International Journal of Molecular Sciences*, 21(23), 9008. <https://doi.org/10.3390/ijms21239008>
- Wild, C., Weiderpass, E., & Stewart, B. (2020). World cancer report: Cancer Research for Cancer Prevention. In Centre international de recherche sur le cancer. International Agency for Research on Cancer. <http://publications.iarc.fr/586> Licence: CC BY-NC-ND 3.0 IGO.
- Xanthoulea, S., Konings, G. F. J., Saarinen, N., Delvoux, B., Kooreman, L. F. S., Koskimies, P., Häkkinen, M. R., Auriola, S., D'Avanzo, E., Walid, Y., Verhaegen, F., Lieuwes, N. G., Caiment, F., Kruitwagen, R., Romano, A., & ENITEC. (2021). Pharmacological inhibition of 17 β -hydroxysteroid dehydrogenase impairs human endometrial cancer growth in an orthotopic xenograft mouse model. *Cancer Letters*, 508, 18–29. <https://doi.org/10.1016/j.canlet.2021.03.019>
- Yan, S., Huang, C., Wu, S., & Yin, M. (2010). Oleanolic acid and ursolic acid induce apoptosis in four human liver cancer cell lines. *Toxicology in Vitro*, 24(3), 842–848. <https://doi.org/10.1016/j.tiv.2009.12.008>